Experimental Evaluation of Tool Run-Out in Micromilling

Aldo Attanasio[1, a)] and Elisabetta Ceretti[1, b)]

[1] *University of Brescia, via Branze 38, 25123 Brescia*
[a)]*Corresponding author: aldo.attanasio@unibs.it*
[b)]*elisabetta.ceretti@unibs.it*

Abstract. This paper deals with micro milling cutting process focusing the attention on tool run-out measurement. In fact, among the effects of the scale reduction from macro to micro (i.e., size effects), tool run-out plays an important role. This research is aimed at developing an easy and reliable method to measure tool run-out in micro milling based on experimental tests and an analytical model. This measuring strategy, from an Industry 4.0 perspective, can be integrated into an adaptive system for controlling cutting forces, with the objective of improving the production quality, the process stability, reducing at the same time the tool wear and the machining costs. The proposed procedure estimates the tool run-out parameters from the tool diameter, the channel width, and the phase angle between the cutting edges. The cutting edge phase measurement is based on the force signal analysis. The developed procedure has been tested on data coming from micro milling experimental tests performed on a Ti6Al4V sample. The results showed that the developed procedure can be successfully used for tool run-out estimation.

Keywords. Micro-milling, tool run-out, experimental test, analytical model, Industry 4.0.

INTRODUCTION

Micro manufacturing processes are becoming fundamental in several industrial fields, such as biomedical, mechanical, automotive and aerospace. Therefore, many researchers are focusing their attention on these processes. The discussion on the definition of "micro manufacturing" is still open. Dornfeld et al. in [1], referring to their modified version of the Taniguchi graph [2], define "micro manufacturing" all the processes which accuracy is lower than one micron. Masuzawa et al. [3] consider as micro manufacturing processes all the processes utilized for producing features that cannot be achieved by conventional processes; while in [4] the production of micro parts is defined as "the production of parts or structures with at least two dimensions in the sub-millimetre". Differently, Alting et al. [5] focused their attention on the definition of micro manufacturing as all the processes dealing with developing and manufacturing components with functional characteristics of at least one dimension of the order of millimetre. It is evident that all these definitions refer to different process issues: feature dimension, process accuracy, surface roughness, feature feasibility, and so on.

A definition covering all the issues characterizing a micro manufacturing process is hard to give, this is because a wide range of different manufacturing processes are used to make micro features and/or micro components. Among these processes, micro cutting or micro mechanical machining processes show some important advantages. They are cost-effectively, flexible, efficient, and it is possible to manufacture complex shape with high removal rate, high accuracy, and good roughness.

When approaching micro cutting operations, phenomena that can be neglected at macro scale become important. Being the tool dimension, the uncut chip thickness and the material grain size of the same order of magnitude, a variation of characteristics from a general behaviour (i.e., size effect) can be observed when reducing the cutting size [6]. Under these working conditions, one of the main issues to be considered is the so called minimum chip thickness value. It is the minimum values of depth of cut under which the removal process is dominated by a ploughing regime instead of shearing one. It was demonstrated that this process parameter is related to the tool material and geometry [7], and the workpiece material and its microstructure [8]. The size effect strongly affects

also the Specific Shear Energy (SSE) needed for material removal. In fact, as reported in [7], SSE increases as the uncut chip thickness decreases.

Being critical in micromilling [9-11] to understand how process parameters (feed per tooth, cutting velocity, and depth of cut), tool geometry (tool edge radius, helix angle, etc.) and the tool-machine pairs (tool-spindle run-out, machine stiffness, etc.) affect the process and the part quality, analytical models, suitable for describing cutting operations in micro-scale, are very helpful. Yoon et al. [12] investigated the influence of tool deflection and radial depth of cut on chip formation in micro milling. An analytical model for estimating unbalanced cutting forces due to tool run-out is proposed by Attanasio et al. [13]. In this model, different force profiles for each cutting edge are considered as a function of the tool run-out and the coefficients of the analytical model are calibrated using the Particles Swarm Optimization algorithm. In their model, Park et al. [14] considered the tool deflection and the tool run-out for the tool trajectories expression. An analytical model for predicting three-dimensional cutting forces of micro end milling process, based on a trochoid trajectory of the cutting edge and tool run-out, was developed by Li et al. [15]. Other works dealing with the development of micro milling cutting force models can be found in literature demonstrating the high interest on this topic. All these papers agree upon the need of including in these models the influence of cutting regimes (ploughing and shearing), trajectory of the cutting edges, tool run-out, tool deflection, elastic recovery, and entry and exit angles.

Among all these influencing factors, the tool run-out plays an important role because in micromilling the ratio between tool run-out and feed per tooth is very high [16]. In some cases the tool run-out is so high that just one flute cuts the material, generating an asymmetric cutting [17].

The objective of this research is to develop an easy and reliable method to measure tool run-out in micromilling. The developed procedure was tested on data coming from experimental tests, consisting in in realizing micro channels 800 µm width by using coated tungsten carbide micro mills on sample made of Ti6Al4V alloy.

GEOMETRICAL MODEL OF TOOL RUN-OUT

Tool run-out is a phenomenon due to the sum of geometrical displacements of spindle axis, tool-holder axis and tool axis from the theoretical rotation axis. These displacements generate a deviation between the theoretical cutting edges trajectory and the actual one.

From a geometric point of view, the tool run-out can be described by four parameters, shown in Figure 1. Two parameters, namely offset distance or run-out length (r_o) and offset or run-out angle (γ_o), define the axis offset; two parameters, namely tilt angle (τ) and location angle of tilt angle (ϕ), define the axis tilt.

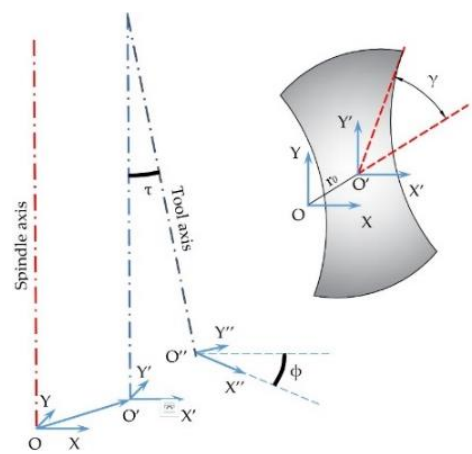

FIGURE 1. Geometric parameters of tool run-out.

Typically, in conventional milling, being the mill diameter very large compared to tool run-out, this error has low influence on the cutting process. Instead, because of the limited tool dimension, in micro milling the tool run-out influence on the process cannot be neglected. In particular, the tool run-out makes unbalanced chip thickness between the mill teeth. This unbalanced load on the teeth generates unavoidable vibrations that affect the process stability. Therefore, to minimize the tool run-out in micro-milling is essential in order to increase the final quality of

the surface finish, to avoid accelerated tool wear or even tool breakage, and to avoid the inception of undesired vibrations (i.e., higher stability of the process).

The proposed geometrical model is based on the hypothesis that the tilt parameters (tilt angle and location angle of tilt angle) can be neglected. This assumption can be done considering that when performing micro machining operations the use of suitable machine tool (i.e., nano precision, ultra precision or high precision machine tool), is strongly recommended. These machine tools guarantee tilt angles lower than a hundredth of degree.

Under this hypothesis the schematization of tool run-out reported in Figure 2a was considered. As shown, the tool run-out is defined by the run-out length (r_o) and the run-out angle (γ_o). Figure 2b shows the expected cutting force signal (one round) in milling when using a two flute micro end mill and in presence of tool run-out.

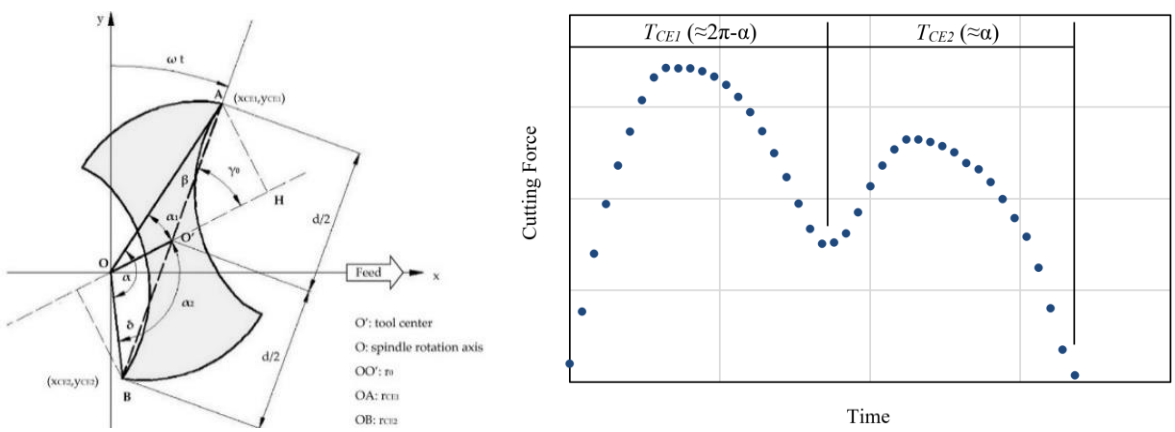

(a) (b)

FIGURE 2. (a) Tool run-out model. (b) A generic experimental signal of cutting force of a two flutes micro-end-mill in presence of tool run-out.

The geometrical model of the cutting edges trajectories of a two flutes micro end-mill considering the tool run-out is fully described in [13] where it was demonstrated that all the equations, which describe the flutes movement, depend on the tool run-out parameters (r_o and γ_o). These parameters can be estimated measuring the actual tool diameter (i.e., AB in Figure 2a), the rotational radius of the first cutting edge (i.e., r_{CE1}=OA in Figure 2a), and the cutting edge phase (i.e., α in Figure 2a). In fact, referring to AOB triangle of Figure 2a and applying the sine law it is possible to compute the values of δ and β angles by using Eq. 1 and Eq. 2.

$$\frac{\overline{AB}}{\sin\alpha}=\frac{\overline{OA}}{\sin\delta} \rightarrow \sin\delta=\frac{\overline{OA}}{\overline{AB}}\cdot\sin\alpha \rightarrow \delta=\arcsin\left(\frac{\overline{OA}}{\overline{AB}}\cdot\sin\alpha\right) \tag{1}$$

$$\beta=\pi-\alpha-\delta \tag{2}$$

Then, applying the law of cosines (Eq. 3), it is possible to calculate the rotational radius of the second cutting edge r_{CE2} ($\overline{OB}$).

$$r_{CE2}=\overline{OB}=\sqrt{\overline{OA}^2+\overline{AB}^2-2\cdot\overline{OA}\cdot\overline{AB}\cdot\cos\beta} \tag{3}$$

Now, referring to BOO' triangle of Figure 2, the tool run-out length r_o (OO') can be obtained utilizing the law of cosines (Eq. 4).

$$r_o=\overline{OO'}=\sqrt{\overline{OB}^2+\overline{O'B}^2-2\cdot\overline{OB}\cdot\overline{O'B}\cdot\cos\delta} \tag{4}$$

While, using the sine law, the tool run-out angle (γ_o) is calculated (Eq. 5).

$$\frac{\overline{OO'}}{\sin\delta}=\frac{\overline{OB}}{\sin\gamma_o} \rightarrow \sin\gamma_o=\frac{\overline{OB}}{\overline{OO'}}\cdot\sin\delta \rightarrow \gamma_o=\arcsin\left(\frac{\overline{OB}}{\overline{OO'}}\cdot\sin\delta\right) \tag{5}$$

Then, it is possible to estimate the tool run-out parameters realizing micro channels and following the procedure reported in Figure 3.

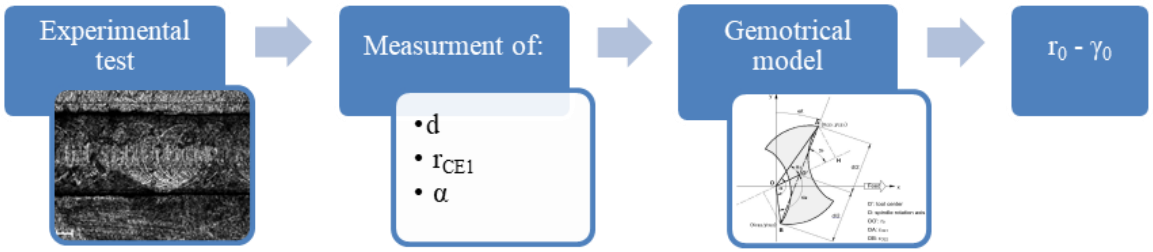

FIGURE 3. The procedure proposed for calculating the tool run-out parameters (r_o and γ_o).

The actual tool diameter (d) can be directly measured from the tool, while, the rotational radius of the first cutting edge (r_{CE1}) can be measured from the channel width, which corresponds to two times this radius. In particular, the tool diameter was measured by using a Hirox RH-2000 confocal microscope while the width of the channels was measured using a Mitaka PF-60 laser probe.

To measure the cutting edge phase (α) is not easy. In this research, an indirect measuring of the cutting edge phase from the cutting force signal was used.

The change of phase of the cutting edges from π to α generates different cutting time for each tooth. Referring to Figure 2b, it is evident that the load and the cutting time of the first cutting edge are higher than that of the second cutting edge. The force signal analysis provides the values of the cutting time of each cutting edge. The cutting time of each tooth depends on cutting edge phase (α) and can be estimated by using Eq. 6 and Eq. 7.

$$T_{CE1}=T\cdot\frac{2\pi-\alpha}{2\pi} \tag{6}$$

$$T_{CE2}=T\cdot\frac{\alpha}{2\pi} \tag{7}$$

Where:

$$T=T_{CE1}+T_{CE2} \tag{8}$$

Is the cutting period.

Then, the cutting edge phase (α) can be derived by Eq. 9.

$$\alpha=2\pi\cdot\frac{T_{CE2}}{T} \tag{9}$$

In order to automate the procedure for the calculation of cutting edge phase (α), Matlab® environment was used. The experimental force signal was approximated using a Fourier series fitting function. Then, a Matlab® script allowed to calculate the cutting time of the first cutting edge (T_{CE1}), the cutting time of the second cutting edge (T_{CE2}), the cutting period (T), and, finally, the cutting edge phase (α). Further details on this procedure are reported in [18].

EXPERIMENTAL SET-UP

The experimental tests consisted in milling micro channels on a Ti6Al4V alloy sample. The sample material was heat treated [10, 11] in order to obtain a fully Widmanstätten or lamellar microstructure. The tests were performed on a five axis Nano Precision Machining Centre KERN Pyramid Nano equipped with a Heidenhain iTCN 530 numeric control. A coated two flutes tungsten carbide micro end mill 800 µm diameter made by SECO (specification SECO-JM905L008-MEGA-T) was used. The PVD coating was nitride of titanium and aluminium, a good material for titanium alloys cutting. A confocal digital microscope (Hirox RH-2000) was used to measure the cutting edge radius obtaining a value of 4 µm. The produced channels consisted in rectangular slots 100 µm depth having a width equal to the tool diameter and a length of 12 mm. Table 1 summarizes the cutting parameters utilized during the tests. The feed per tooth was selected according to the tool data sheet. In particular, a value higher than the cutting edge radius was chosen in order to avoid ploughing regime.

TABLE 1. Cutting condition utilized during the experimental tests.

Parameter	Value
Cutting Speed	10.5 m/min
Spindle speed	4166 rpm
Feed per tooth (f_z)	10 µm/tooth
Axial depth of cut (a_p)	100 µm
Radial depth of cut (a_e)	Tool diameter
Lubrication	Dry

During the experimental phase the same tool was used. At the end of each cut, the tool-holder was unmounted from the spindle for checking the tool in order to assure that the tool wear did not affect the cutting force. Due to the low cutting length, no evidence of tool wear was highlighted during controls. In particular, it was checked that the cutting edge radius was constant (4 µm) during all the tests, because an excessive increase of the cutting edge radius can change the cutting regime from shearing to ploughing. Then, the tool holder, rotated of ninety degrees, was mounted on spindle and a new channel was produced. In this manner, the tool run-out randomly changes for each test. Four channels were made applying this procedure, obtaining four different run-out conditions (i.e., Test 0, Test 90, Test 180, and Test 270). Figure 4 shows the measured cutting force component along the Y-axis for each test. The higher tool run-out was observed for Test 180 (Figure 4c), while the lower for Test 270 (Figure 4d).

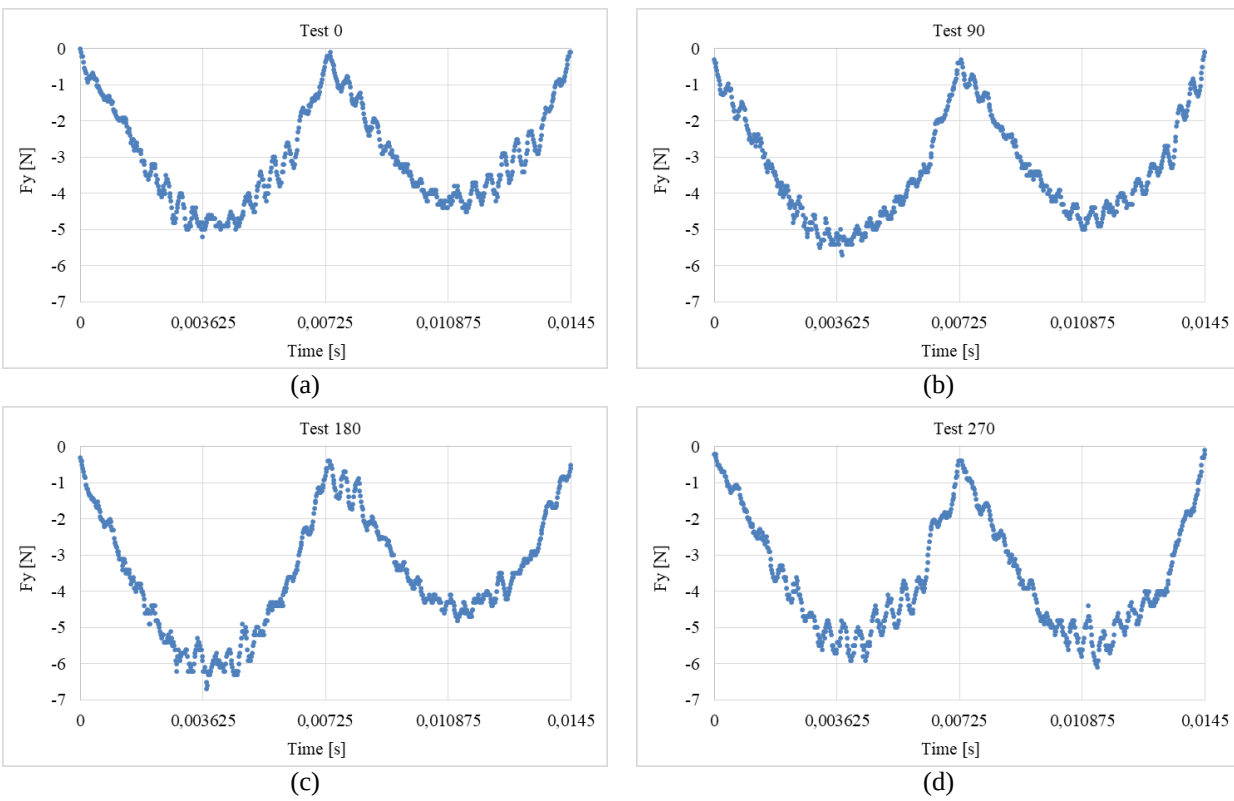

FIGURE 4. Cutting force component along Y-axis. (a) Test 0; (b) Test 90; (c) Test 180; (d) Test 270.

RESULTS

Table 2 reports the R-square goodness-of-fit statistic, the cutting time of the first cutting edge (T_{CE1}), the cutting time of the second cutting edge (T_{CE2}), the cutting period (T), and the cutting edge phase (α) obtained from the cutting force analysis. The high value of the R-square goodness-of-fit statistics confirms the suitability of the Fourier series fitting functions in correctly representing the cutting force signal. In Table 2 the tool run-out parameters value

(r_O and γ_O) obtained applying the proposed procedure are also reported. The results provided by the proposed procedure are in agreement with the measured cutting force (Figure 4). In fact, the higher run-out parameters were calculated for Test 180, the lower for Test 270.

TABLE 2. Fourier series fitting function results: R-square, T_{CE1}, T_{CE2}, T, α, r_o, and γ_o.

Parameter	Test 0	Test 90	Test 180	Test 270
R-square	0.9645	0.9781	0.9740	0.9737
T_{CE1} [s]	0.007347	0.007334	0.007541	0.007308
T_{CE2} [s]	0.007153	0.007166	0.006959	0.007192
T [s]	0.014500	0.014500	0.014500	0.014500
α [°]	182.4	182.1	187.2	181.4
r_O [μm]	8.77	7.55	25.36	5.29
γ_O [°]	-74.0	-75.2	-86.9	-72.2

CONCLUSIONS

Purpose of this activity has been to design and develop a procedure that was able to measure the tool run-out length and angle parameters overcoming the limits of the actual measuring strategies based on the use of microscopes, laser or interferometers. A geometric model, involving the tool diameter, the channel width and the cutting edge phase, was introduced. For the automatic estimation of the cutting edge phase the cutting edge force signal was processes through a procedure based on fitting curve application of Matlab®. Limits of this procedure are due to the accuracy of the measuring systems used for estimating the tool dimeter and the channel width. For this reason, measuring instruments with high accuracy were used. The results obtained applying this procedure on experimental data demonstrated the possibility of calculating the run-out parameters with a good accuracy.

REFERENCES

1. D. Dornfeld, B. Denkena and G. Byrne, CIRP Annals **52/2**, 483-507 (2003).
2. N. Taniguchi, CIRP Annals **32/2**, 573-582 (1983).
3. T. Masuzawa and H.K. Toenshoff, CIRP Annals **46/2**, 621-628 (1997).
4. M. Geiger, M. Kleiner, R. Eckstein, N. Tiesler and U. Engel, CIRP Annals **50/2**, 445-462 (2001).
5. L. Alting, F. Kimura, H.N. Hansen and G. Bissacco, CIRP Annals **52/2**, 635-657 (2003).
6. A.J. Mian, "Size effect in micromachining", Ph.D. thesis, The University of Manchester, 2011.
7. X. Lai, H. Li, C. Li, Z. Lin and J. Ni, Int. J. Mach. Tools Manuf. **48/1**, 1-14 (2008).
8. T. Komatsu, T. Yoshino, T. Matsumura and S. Torizuka, Procedia CIRP **1**, 150-155 (2012).
9. K. Monroy, A. Attanasio, E. Ceretti, H.R. Siller, N. Hendrichs and C. Giardini, Materials **6/4**, 1434-1451 (2013).
10. A. Attanasio, M. Gelfi, A. Pola, E. Ceretti and C. Giardini, Materials **6/9**, 4268-4283 (2013).
11. M. Gelfi, A. Attanasio, E. Ceretti, A. Garbellini and A. Pola, Mat. and Manuf. Proc. **31/7**, 919-925 (2016).
12. M.C. Yoon and Y.G. Kim, J. Mater. Process. Technol. **155-156**, 1383-1389 (2004).
13. A. Attanasio, A. Garbellini, E. Ceretti and C. Giardini, Int. J. Nanomanuf. **11/5-6**, 275-296 (2015).
14. S.S. Park and M. Malekian, CIRP Annals **58/1**, 49-52 (2009).
15. C. Li, X. Lai, H. Li and J. Ni, J. of Micromech. and Microeng. **17**, 671-678 (2007).
16. K. Li, K. Zhu and T. Mei, Int. J. Mach. Tools Manuf. **105**, 23–31 (2016).
17. P. Rodríguez and J.E. Labarga, J. Mater. Process Technol. **213/2**, 261-268 (2013).
18. A. Attanasio, Micromachines **8**, 221-236, (2017).